Materials & Design 254 (2025) 114130

Contents lists available at ScienceDirect

Materials & Design

journal homepage: www.elsevier.com/locate/matdes

Enhanced ferroelectric performance in $Hf_{0.5}Zr_{0.5}O_2$ capacitors using ultra-thin MoS_2 layer for clamping effect and oxygen vacancy suppression

Soyeon Lee [a,1], Hyun Woo Jeong [b,1], Jun-Cheol Park [a], Donghyeon Lee [a], Yong-Ryun Jo [c], Jiwoong Yang [a], Min Hyuk Park [b,*], Sanghan Lee [a,d,*]

[a] Department of Materials Science and Engineering, Gwangju Institute of Science and Technology (GIST), 123 Cheomdangwagi-ro, Buk-gu, Gwangju 61005, Republic of Korea

[b] Department of Materials Science and Engineering, College of Engineering, Seoul National University, Gwanak-ro 1, Gwanak-gu, Seoul 0882, Republic of Korea

[c] GIST Advanced Institute of Instrumental Analysis (GAIA), Electron Microscopy Laboratory, Gwangju Institute of Science and Technology (GIST), 123 Cheomdangwagi-ro, Buk-gu, Gwangju 61005, Republic of Korea

[d] Research Institute for Solar and Sustainable Energies (RISE), Gwangju Institute of Science and Technology (GIST), 123, Cheomdangwagi-ro, Buk-gu, Gwangju 61005, Republic of Korea

ARTICLE INFO

Keywords:
$Hf_{0.5}Zr_{0.5}O_2$
Ferroelectric capacitor
Two-dimensional metal chalcogenides capping layer
Clamping effect
Oxygen vacancy suppression

ABSTRACT

Since the discovery of ferroelectric properties in HfO_2-based thin films, capping effect has been extensively researched to induce ferroelectric orthorhombic phase through mechanical clamping. However, current research on capping materials has focused on oxide-based materials to address wake-up effect resulted from 3D metallic capping electrodes, yet the challenge of achieving a large double remnant polarization value remains unresolved. Here, ultra-thin (≈ 1 nm) MoS_2, one of transition metal dichalcogenides, was employed as a novel capping layer on $Hf_{0.5}Zr_{0.5}O_2$ thin films. Notably, MoS_2-capped $Hf_{0.5}Zr_{0.5}O_2$ films exhibited a higher orthorhombic phase fraction than uncapped films, resulting in an enhanced double remnant polarization value of ≈ 42.2 μC cm^{-2}. This represents approximately a three-fold increase compared to the uncapped $Hf_{0.5}Zr_{0.5}O_2$ films (≈ 14.8 μC cm^{-2}), attributed to volumetric suppression via the clamping effect even with ultra-thin capping. Additionally, the MoS_2-capped $Hf_{0.5}Zr_{0.5}O_2$ device exhibited enhanced cycling limits (>10^6 cycles), achieved by suppressed oxygen vacancies at the top electrode-$Hf_{0.5}Zr_{0.5}O_2$ film interface, thanks to the dangling bond-free nature of transition metal dichalcogenides. This study demonstrates that ultra-thin MoS_2 effectively functions as a capping layer, enhancing both remnant polarization and endurance for 1T-1C FeRAM applications while preserving the scalability of $Hf_{0.5}Zr_{0.5}O_2$.

1. Introduction

Since the discovery of ferroelectric (FE) properties in HfO_2 thin films in 2011 [1], extensive research has focused on HfO_2 due to its scalability and compatibility with complementary metal-oxide semiconductor (CMOS) technology [2,3]. In particular, doped HfO_2 thin films with enhanced FE properties have garnered significant attention as promising candidates for FE-based non-volatile memory devices such as one-transistor one–capacitor (1T-1C) ferroelectric random-access memory (FeRAM) and ferroelectric field effect transistor (FeFET). Among various dopants such as Al, Gd, Zr, Y, and La, Zr-doped HfO_2 has been intensively studied due to its relatively lower processing temperature and stable FE response, attributed to the similar physical and chemical properties of HfO_2 and ZrO_2 [4–8]. However, the practical utilization of $Hf_xZr_{1-x}O_2$ thin films as a capacitor in 1T-1C FeRAMs is challenged by their insufficient double remnant polarization ($2P_r$) value, which hinders the achievement of a large memory window, low leakage current, and uniform FE properties over multiple operating cycles [9–12]. Given that a $2P_r$ value of approximately 30 μC cm^{-2} is required for reliable FeRAMs, improving polarization performance is essential [13–15].

With varying doping ratio of Zr in HfO_2, $Hf_{0.5}Zr_{0.5}O_2$ (HZO) exhibits diverse characteristics, such as dielectric, ferroelectric, and antiferroelectric properties, which correspond to the monoclinic (m-phase, space group: $P2_1/c$), orthorhombic (o-phase, space group: $Pca2_1$), and

* Corresponding authors at: Department of Materials Science and Engineering, Gwangju Institute of Science and Technology (GIST), 123 Cheomdangwagi-ro, Buk-gu, Gwangju 61005, Republic of Korea (S. Lee).

E-mail addresses: minhyuk.park@snu.ac.kr (M.H. Park), sanghan@gist.ac.kr (S. Lee).

[1] These authors contributed equally.

https://doi.org/10.1016/j.matdes.2025.114130
Received 25 January 2025; Received in revised form 16 May 2025; Accepted 20 May 2025
Available online 21 May 2025

tetragonal (t-phase, space group: $P4_2/nmc$) phases, respectively [3,5,6,16,17]. The o-phase, which is the origin of ferroelectricity due to its non-centrosymmetric property, exists in a metastable state. Since early studies, applying a 3D metallic capping electrode on HZO thin films has been tremendously reported as an effective method to enhance the areal fraction of the FE o-phase by suppressing the volumetric expansion of the t-phase during the annealing process. This leads to inhibition of the phase transition from the t-phase to the m-phase [18–21], a phenomenon referred to as the "Clamping Effect" [22–25]. However, the wake-up effect, the increase in polarization with field cycling, occurs when applying a 3D metallic capping electrode [26–28]. Various factors such as phase transformation, domain depinning, ferroelastic domain switching, and breakdown of the dielectric interfacial layer have been associated with this effect [29–31]. However, the wake-up effect is primarily attributed to domain depinning caused by the redistribution of charged oxygen vacancies (V_o) at the interface between the HZO film and the top electrode. These vacancies result from unwanted interface reactions and oxygen scavenging during the deposition process or post-metallization annealing of FE films [3,26–28,32]. The unstable FE cyclic characteristic causes hard breakdown and deterioration of operation parameters such as the read/write voltages of FeRAM, posing a significant obstacle to their stable and long-term use [12]. Thus, numerous research on capping layers for HZO thin films has been focused on the suppression of V_o to overcome this reliability limitation.

Zhang et al. reported enhanced endurance and retention properties by supplying oxygen at the interface of electrode-HZO film using VO_x capping, which has a lower bond energy of V–O compared to that of the Hf–O [33]. Onaya et al. found that ZrO_2 interfacial layer induced wake-up free properties by inhibiting the oxygen scavenging at TiN top electrode [34]. Additionally, Goh et al. demonstrated a V_o-suppressed interface using RuO_2 top electrode, which provides additional oxygen to the HZO layer, resulting in a reduced wake-up effect [35]. These results indicate that interface engineering to prevent unwanted reactions is crucial for achieving reliable cyclic characteristics with prolonged endurance cycles.

Meanwhile, at present, there have been limitations in the $2P_r$ value in some studies, possibly due to insufficient clamping effects, since research on capping materials has been limited to oxide-based materials to primarily address V_o suppression [34,36,37]. Since large $2P_r$ value is crucial for high-performance 1T-1C FeRAMs, novel capping materials that not only effectively induce large fraction of the FE o-phase via mechanical stress but also reduce the amounts of defects at the interface are required.

Two-dimensional (2D) transition metal dichalcogenides (TMDs) suppress unwanted interfacial interactions due to their unique property of dangling bond-free surface, which inhibits the formation of V_o and ensures a clean interface [38,39]. Additionally, despite the presence of van der Waals (vdW) bonding resulting from the absence of dangling bonds on the surface [38,40], it has been demonstrated that ultrathin monolayer TMDs effectively sustain strain both theoretically and experimentally [41], which opens up the possibility of inducing a clamping effect using ultra-thin TMDs as a capping layer. These make TMDs unique as capping materials, enhancing both endurance characteristics and ferroelectric properties through the use of an extremely thin layer, which has yet to be studied.

In this study, we introduce a unique capping layer of molybdenum disulfide (MoS_2) to enhance both ferroelectricity and reliability of ferroelectric capacitors in 1T-1C FeRAMs. The MoS_2 capping layer exhibited a strong clamping effect by effectively inhibiting the formation of the non-FE m-phase, thereby enhancing the areal fraction of the FE o-phase. Consequently, the $2P_r$ value of MoS_2-capped HZO film was 42.2 μC cm^{-2}, representing approximately a three-fold increase compared to uncapped HZO capacitor ($2P_r \approx 14.8$ μC cm^{-2}). Furthermore, the dangling bond-free nature of 2D TMDs resulting in decreased amount of V_o at the interface compared to the uncapped HZO capacitor. Notably, owing to the ability to enhance both of $2P_r$ value and endurance properties via interface engineering with ultrathin (≈ 1 nm) MoS_2 layer, MoS_2-capped HZO capacitors preserve their superior advantages of scaling down.

2. Experimental methods

2.1. Device fabrication

The TiN bottom electrodes were deposited to a thickness of 50 nm on a Si substrate using radio frequency (RF) magnetron sputtering (Co-sputtering system, DAEKI HI-TECH). The sputtering conditions included a power of 200 W, working pressure of 1 mTorr, and an Ar flow rate of 20 sccm. The HZO thin films were deposited to a thickness of 10 nm using atomic layer deposition (ALD, Atomic classic, ISAC Research) at a temperature of 280 °C. During the ALD process, $[(CH_3)(C_2H_5)N]_4Hf$ (TEMAHf), $[(CH_3)(C_2H_5)N]_4Zr$ (TEMAZr) and O_3 served as the Hf-precursor, Zr-precursor, and reactant, respectively. For capped samples, approximately 1 nm of MoS_2 was subsequently grown using commercial target (LTS Research Laboratories, Inc.) via pulsed layer deposition (PLD) equipped with a KrF ($\lambda = 248$ nm) excimer laser (Coherent, COMPex PRO 205F). The laser energy density, substrate temperature, and repetition rate were set at 1.3 J·cm^{-2}, 500 °C, and 3 Hz, respectively, when operating pressure was maintained at 100 mTorr with an Ar flow of 50 sccm. To crystallize the HZO thin films, rapid thermal annealing (RTA) was conducted at 500 °C for 60 s under an N_2 gas atmosphere at 100 mTorr. Finally, 50-nm-thick Pt top electrodes were deposited by e-beam evaporation through a shadow mask with a hole diameter of ≈ 120 μm for patterning.

2.2. Device electrical measurement

Electrical characterizations were performed using a TF analyzer measurement system (TFA 3000, Aixacct). Polarization-electric field (P-E) and current density–electric field (J–E) curves were obtained by applying a bipolar triangular pulse with various voltage amplitudes at a frequency of 1 kHz. Positive up negative down (PUND) measurements were conducted to measure the ferroelectric response while eliminating non-ferroelectric components with rising and falling pulses, with delay times set to 250 μs, between ±4.5 V. For the endurance test, a bipolar rectangular pulse between ±4.5 V at a frequency of 50 kHz was used. Leakage current-electric field measurements were conducted after applying a pre-pooling voltage pulse of −2 V for 1 s. The current was measured while applying a staircase voltage between −2 V and 2 V in 0.1 V steps for 1 s. ε_r (relative permittivity)-V(voltage) measurements were performed after applying a pre-poling voltage pulse of −4 V. Capacitance and loss tangent were measured while applying a small signal at 100 staircase voltage steps, with the frequency set to 10 kHz and the amplitude to 50 mV (Fig. S1).

2.3. Material characterization

Raman spectroscopy (InVia, Renishaw) with the laser wavelength of 514.5 nm was employed for the structural analyses of the MoS_2 capping layer. Structural analyses of HZO thin films were carried out using grazing incidence X-ray diffraction (GIXRD, Smart Lab, Rigaku) with a Cu-Kα source ($\lambda = 1.5406$ Å), and high-resolution transmission electron microscopy (HR-TEM, Tecnai G2 F30 S-Twin, FEI). X-ray photoelectron spectroscopy (XPS, NEXSA, Thermo Fisher Scientific, monochromatic Al-Kα source) measurements were performed to investigate V_o at the interface, with the binding energy of the XPS spectra calibrated using the 284.5 eV C signal.

3. Results and discussion

Fig. 1 illustrates the schematic structures of the HZO capacitors

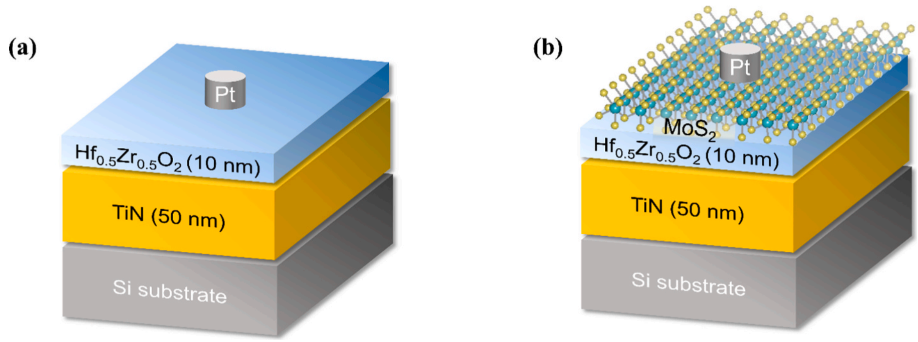

Fig. 1. Schematic illustrations of fabricated metal-ferroelectric-metal (MFM) capacitors; (a) MoS_2-uncapped (w/o MoS_2) and (b) MoS_2-capped (w/ MoS_2) HZO capacitor.

without MoS_2 capping and with ultra-thin MoS_2 capping. Fig. 2a presents the grazing incident X-ray diffraction (GIXRD) patterns of each capacitor. Due to the extreme thinness of MoS_2 ($\approx$ 1 nm), the peak of MoS_2 was not observed in GIXRD results. Therefore, Raman spectra in the range of 355–445 cm^{-1} and XPS spectra of Mo 3d and S 2p were measured to verify the presence of the MoS_2 layer, as shown in Fig. S2-3, respectively. In Fig. 2a, GIXRD patterns of each HZO film are shown. The peak at $\approx$ 30.5° is generally attributed to the (1 1 1) peak from the FE o-phase and the (1 0 1) peak from the non-FE tetragonal phase (t-phase), while the peaks at $\approx$ 28.6° and $\approx$ 31.7° correspond to the (−1 1 1) and (1 1 1) peaks from the non-FE m-phase [36,42,43]. To quantitatively analyze the phase fraction of HZO, comparing the relative peak areas of the o/t-phase and m-phase is effective [13]. Fig. 2b shows Gaussian-fitted GIXRD curves in the 2θ range of 27°–33° from Fig. 2a, and Fig. 2c summarizes the phase fraction of the HZO films. From Gaussian fitting, it was observed that the non-FE m-phase fraction significantly decreased from 59 % to 35 % in MoS_2-capped HZO film. Consequently, the o/t-phase fraction increased, indicating that MoS_2 capping layer sufficiently inhibits the non-FE m-phase by suppressing volumetric expansion through mechanical clamping.

Fig. S4 shows the ε_r (relative permittivity)-V (voltage) curves of the MoS_2-uncapped and capped HZO capacitors. The MoS_2-capped HZO capacitor exhibited a higher ε_r value than the uncapped HZO capacitor. Since the o-phase has a higher ε_r value compared to the m-phase [44], this result might suggest that the MoS_2-capped HZO film had a larger areal fraction of the o-phase, consistent with GIXRD results.

To further clearly investigate the impact of MoS_2 on the FE o-phase fraction, high resolution-transmission electron microscopy (HR-TEM) analyses were performed. Fig. 3a and b display the cross-sectional HR-TEM images of the MoS_2-uncapped and capped HZO films, respectively. Notably, as shown in Fig. 3b, the presence of uniformly formed MoS_2 layer was verified with a thickness of 1 nm. For better visibility, the reverse fast Fourier transformation (FFT) images were generated by filtering FFT images with masks. In the FFT images, the inter-atomic distance (*d*) spacing values were measured to determine the phase information. Each colored box and corresponding region in HR-TEM images represents different phases identified in the FFT images. Through multiple analyses of various regions, we observed that the (1 1 1)-oriented and the (1 1 0)-oriented m-phase were mainly present in the uncapped HZO film, highlighted in orange and yellow, respectively, with low fraction of (2 0 0)-oriented o-phase, highlighted in green. Conversely, the MoS_2-capped HZO film predominantly displayed the o-phase with orientations (1 1 1) and (2 0 0), colored in blue and green, respectively. Given that the substrate-normal directional phases differed between the MoS_2-uncapped and capped HZO films (m(1 1 1) and o(1 1 1), respectively), it is evident that a larger o-phase fraction was induced through MoS_2 capping. This further confirms the clamping effect of the ultra-thin MoS_2 capping layer, in agreement with the GIXRD results.

Before examining the effect of MoS_2 capping on FE properties of HZO capacitors, it was verified that the MoS_2 deposition temperature of 500 °C in PLD did not have an additional annealing effect beyond RTP (Fig. S5). To investigate the FE performance of the HZO capacitors, polarization-voltage (P-V) loops and the current density–voltage (J–V) curves were measured. Since uncapped HZO capacitors exhibited sharper hysteresis loop at each 10^3 cycles in Figs. S6 and S7, after applying wake-up cycles 10^3 times at a voltage of 4.5 V, all electrical

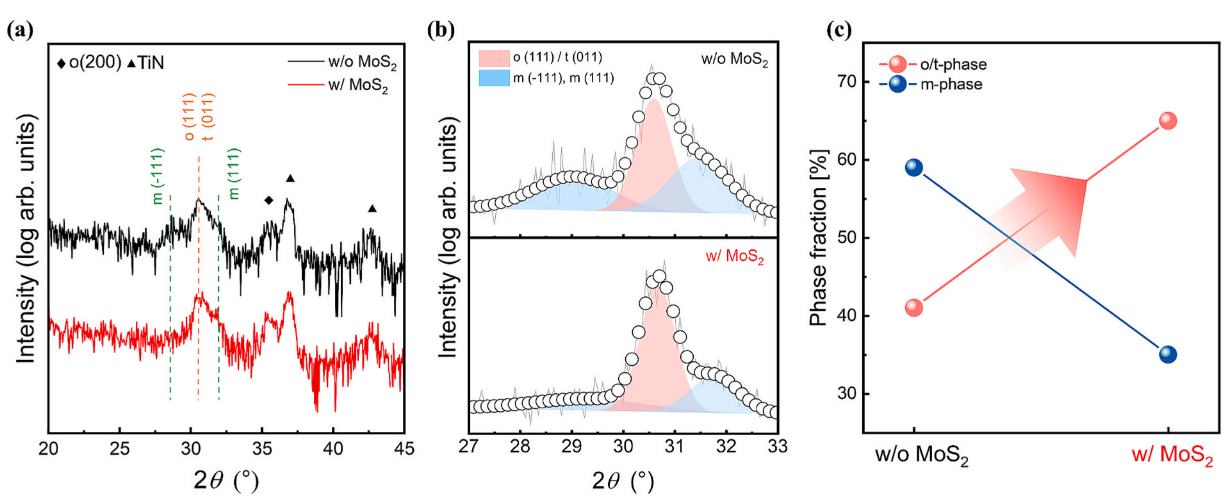

Fig. 2. Structural analyses of MoS_2-uncapped (w/o MoS_2, black) and capped (w/MoS_2, red) HZO films. (a) XRD patterns. (b) Gaussian-fitted XRD patterns from 27° to 33°. (c) Phase fraction of o/t-phase and m-phase from 27° to 33° extracted from XRD by Gaussian fitting. (For interpretation of the references to colour in this figure legend, the reader is referred to the web version of this article.)

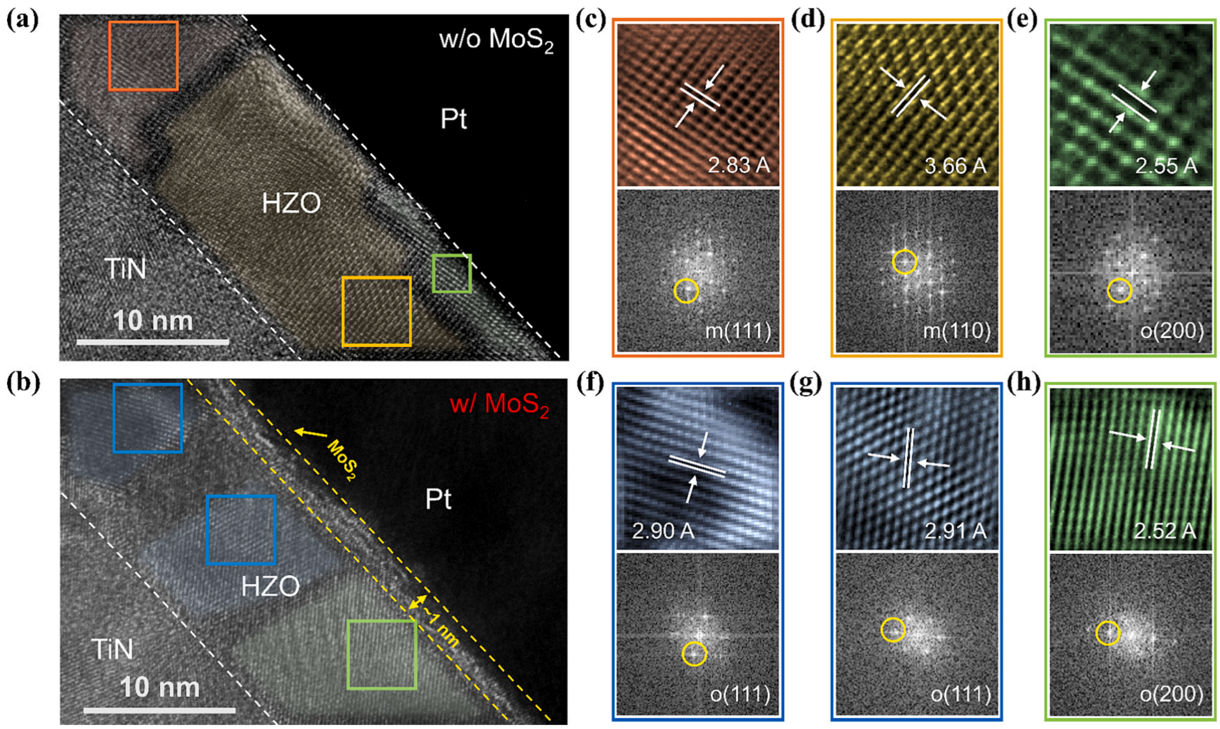

Fig. 3. Cross-sectional HR-TEM images of HZO films for (a) MoS_2-uncapped (w/o MoS_2) and (b) MoS_2-capped (w/MoS_2) HZO films. Each colored box and corresponding region in the HR-TEM images represents different phases identified in the FFT images for (c) m(1 1 1), (d) m(1 1 0), (e) and (h) o(2 0 0), and (f) and (g) o(1 1 1).

characterizations were compared in the operating voltage range of ±3.0 ~ ±4.5 V as shown in Fig. 4. In Fig. 4a, MoS_2-capped HZO capacitor showed larger $2P_r$ value than the uncapped HZO capacitor for all voltage range. Notably, the MoS_2-capped HZO capacitor showed an enhanced $2P_r$ value of 42.2 μC cm^{-2}, which is approximately a three-fold increase compared to the uncapped HZO capacitor (14.8 μC cm^{-2}) between ±4.5 V (Fig. 4b). In the uncapped HZO capacitor, the post-deposition annealing likely increases the fraction of the non-ferroelectric monoclinic phase, which in turn elevates the coercive voltage by inhibiting complete ferroelectric switching [3,45]. In the MoS_2-capped HZO capacitor, part of the applied voltage drops across the MoS_2 layer, reducing the field across HZO. As a result, a higher external voltage is needed to switch the polarization, consistent with reports that interfacial layers increase the coercive voltage in ferroelectric films [46,47]. To determine the intrinsic polarization response without the leakage current effect, P-V loops were measured using the positive-up-negative-down (PUND) method. The MoS_2-capped HZO capacitor exhibited more than a three-fold increase in $2P_r$ value, reaching 35.2 μC cm^{-2} compared to the uncapped HZO capacitor (10.2 μC cm^{-2}) as shown in Fig. 4c, confirming the significant improvement in intrinsic ferroelectricity via MoS_2 capping. Note that these results are consistent with the structural analyses, which observed a notably increased o-phase fraction from GIXRD and a dominant o-phase from HR-TEM. It is remarkable that the MoS_2-capped device showed a noticeable ferroelectricity with thinner capping layer, compared to reported studies (Table S1).

To assess the impact of MoS_2 capping on reliability, endurance tests were conducted with fatigue pulses between ±4.5 V with 50 kHz by extracting $2P_r$ values from PUND tests. As shown in Fig. 5a–c, MoS_2-

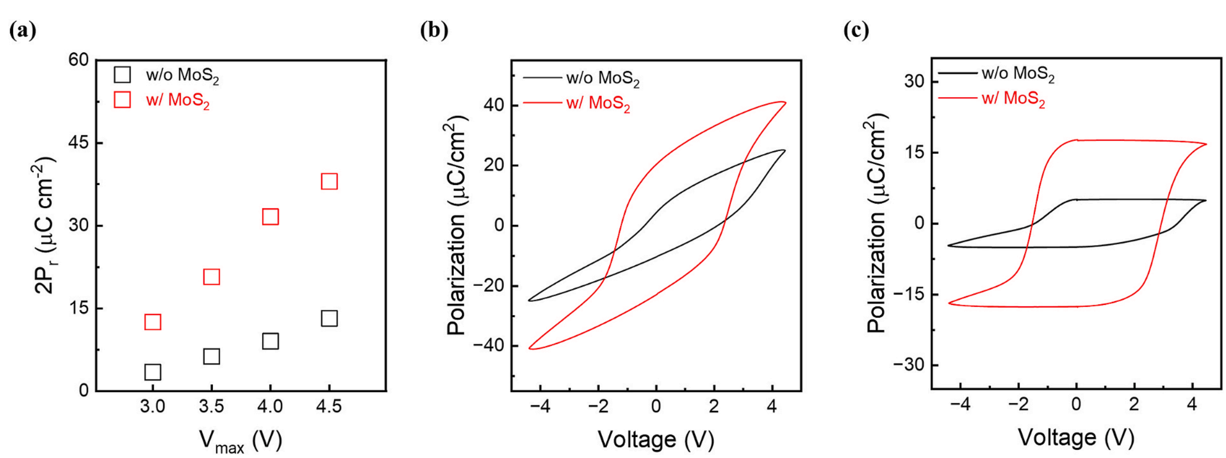

Fig. 4. Comparisons of electrical characterizations of MoS_2-uncapped (w/o MoS_2, black) and MoS_2-capped (w/ MoS_2, red) HZO capacitors. (a) Plots of the $2P_r$ values as a function of V_{max} extracted from PUND measurements using bipolar pulses between ±3.0 ~ 4.5 V, (b) normal P-V curves, and (c) positive up negative down (PUND) P-V curves. (For interpretation of the references to colour in this figure legend, the reader is referred to the web version of this article.)

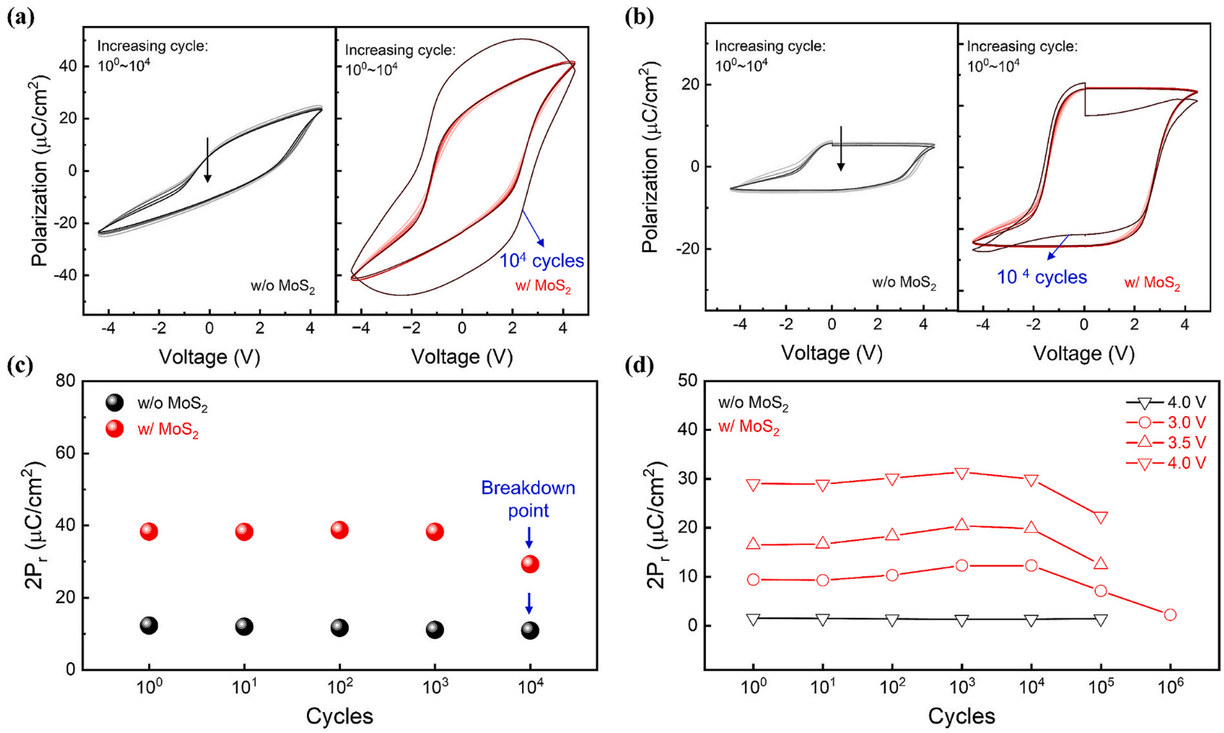

Fig. 5. Endurance test results of MoS_2-uncapped (w/o MoS_2, black) and MoS_2-capped (w/MoS_2, red) HZO capacitors. Bipolar triangle pulses between ±4.5 V was used up to 10^4 switches for (a) normal P-V curves, and (b) positive up negative down (PUND) P-V curves. (c) Plots of the $2P_r$ values as a function of cycle numbers extracted from PUND measurements. (d) Plots of the $2P_r$ values as a function of cycle numbers extracted from PUND measurements using bipolar pulses between ±3.0 V ~ ±4.5 V. (For interpretation of the references to colour in this figure legend, the reader is referred to the web version of this article.)

capped HZO capacitor demonstrated enhanced $2P_r$ value across all operating cycles, confirming robust FE performance via MoS_2 capping. Moreover, the endurance of MoS_2-capped HZO capacitor improved up to 10^4 cycles despite the commonly studied trade-off between the $2P_r$ value and reliability [48]. In Fig. 5d, endurance tests were also conducted with fatigue pulses from ±3.0 V to ±4.0 V to depict polarization switching depending on the voltage (Fig. S8). Notably, at ±3.0 V, the MoS_2-capped HZO capacitor exhibited not only FE full switching characteristics but also enhanced endurance cycles up to 10^6. In contrast, the uncapped HZO capacitor displayed only dielectric properties at ±4.0, reaching up to 10^5 cycles. Although the MoS_2-capped HZO capacitor's polarization decreases significantly after 10^5 switching cycles at ±4.0 V ($2P_r \approx 22.4$ μC cm^{-2}), it still remains higher than that of the uncapped HZO capacitor at the same cycle count ($2P_r \approx 7.1$ μC cm^{-2}), highlighting

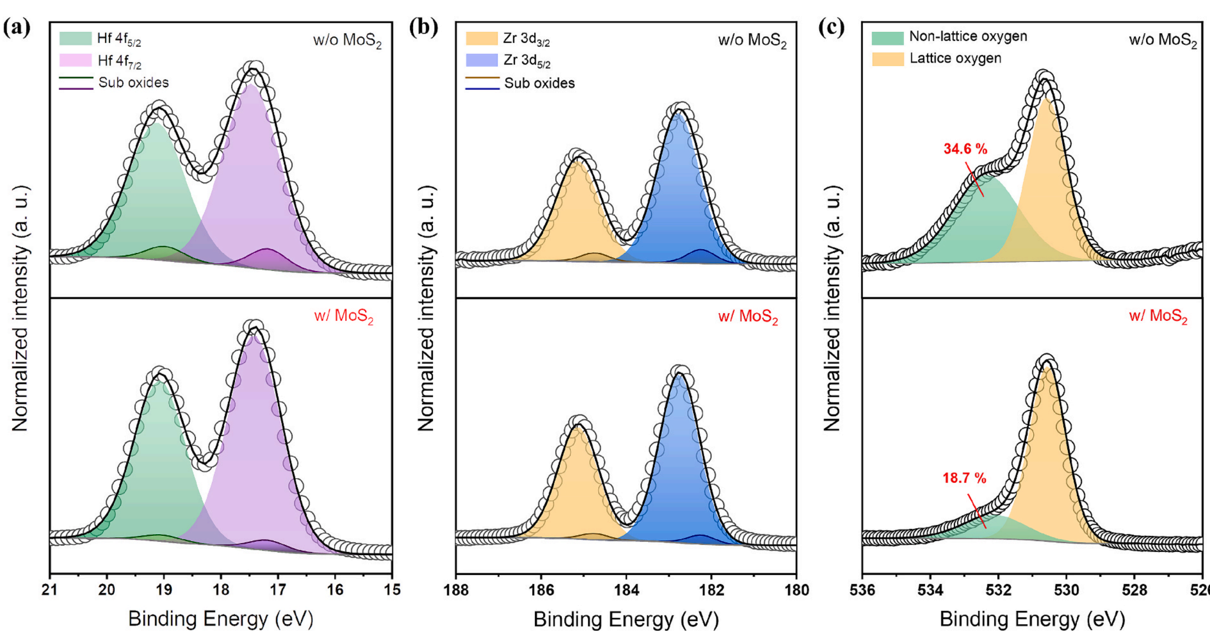

Fig. 6. Representative (a) Hf 4f, (b) Zr 3d, and (c) O 1s XPS spectra for investigation of oxygen vacancies at the interface between HZO film and capping layer of Pt and MoS_2, for MoS_2-uncapped (w/o MoS_2, black) and MoS_2-capped (w/ MoS_2, red) HZO films, respectively. (For interpretation of the references to colour in this figure legend, the reader is referred to the web version of this article.)

meaningful endurance improvement provided by the ultra-thin MoS_2 capping layer. This further confirms that MoS_2 capping induces robust FE properties even at lower voltages, even with enhancing the endurance cycles. Given the general belief that the formation of V_o at the interface between the HZO film and the electrodes is responsible for endurance failure during cycling, MoS_2 capping might reduce the amount of V_o at the interface. [26,27,35,49].

To carefully compare the interfacial interaction related to V_o for both capacitors, x-ray photoelectron spectroscopy (XPS) analysis was carried out using two samples of Pt-capped and MoS_2-capped HZO films for uncapped, and capped HZO capacitors, respectively. The thickness for Pt and MoS_2 were ≈ 1-nm-thick to exclude the effect of thickness on the formation of defects. Given that sub oxides are regarded as chemical species having an intermediate oxidation state containing less oxygen than the corresponding oxide [50–52], the reduced sub oxides ratio in the Hf 4f and Zr 3d spectra of the MoS_2-capped HZO sample suggests a suppressed V_o fraction at the interface (Fig. 6a and b). More remarkably, relative areal ratio of the non-lattice oxygen in the HZO films decreased from 34.6 % to 18.7 % after MoS_2 capping (Fig. 6c). It should be noted that the relative areal ratio does not mean the accurate quantitative fraction of oxygen vacancies because the intensity in XPS is strongly depth-dependent. However, the lower areal ratio of non-lattice oxygen observed for the MoS_2-capped sample supports the decreased relative concentration of V_o in MoS_2-capped HZO sample compared to that of the uncapped HZO sample [12,53–55]. These results suggested that the maintained endurance properties in capped HZO capacitor might be attributed to the suppression of V_o at the interface by inhibiting unwanted interfacial interactions with electrodes via MoS_2 capping layer, which is free of dangling bonds [38,39].

Modeling could further elucidate the how an increase in ferroelectricity, induced by mechanical property modifications, facilitates lower voltage operation and enhances reliability. In the presence of a capping layer, it is known that the annealing process suppresses out-of-plane expansion, resulting in an increase in in-plane tensile stress [21]. Furthermore, when an in-plane tensile strain of 2–2.5 % is applied to HZO thin films, ferroelectricity increases by 34 %, as indicated by DFT calculations [56]. For future studies, DFT-based modeling of HZO could further aid in capacitor structure design by analyzing the effects of capping layers on the polarization and endurance properties [57,58].

Beyond the demonstrated improvements in $2P_r$ and endurance, the possibility of tuning the optoelectronic behavior of MoS_2 via the ferroelectric polarization of HZO suggests its potential for in-memory computing applications [59,60].

4. Conclusion

In summary, we investigated the significant impact of novel MoS_2 capping layer in enhancing ferroelectric properties of HZO films. The ultra-thin (≈ 1 nm) MoS_2 successfully acted not only as a clamping layer but also as a V_o suppression layer on the HZO film. Mechanical confinement via the MoS_2 layer resulted in the inhibition of the m-phase and, thus, an increase in the areal fraction of the FE o-phase in the HZO film. Consequently, a notably enhanced $2P_r$ value (≈ 42.2 μC cm^{-2}) was obtained in the MoS_2-capped HZO capacitor, representing approximately a three-fold increase compared to the HZO capacitor (≈ 14.8 μC cm^{-2}). Additionally, the MoS_2 capping layer suppressed V_o, which is detrimental to endurance properties, by inhibiting unwanted interfacial reaction with dangling bond-free nature, resulting in maintained reliability. Our approach of adopting unique MoS_2 capping layer, which notably enhances the intrinsic $2P_r$ value despite ultra-thinness, may benefit the application of high-performance capacitors in 1T-1C FeRAMs, while maintaining scaling down capability of $Hf_{0.5}Zr_{0.5}O_2$.

CRediT authorship contribution statement

Soyeon Lee: Writing – original draft, Methodology, Investigation, Data curation, Conceptualization. **Hyun Woo Jeong:** Writing – review & editing, Methodology, Investigation, Formal analysis, Data curation. **Jun-Cheol Park:** Writing – review & editing, Investigation, Formal analysis. **Donghyeon Lee:** Methodology, Investigation, Conceptualization. **Yong-Ryun Jo:** Formal analysis, Data curation. **Jiwoong Yang:** Methodology, Data curation. **Min Hyuk Park:** Writing – review & editing, Supervision, Project administration, Funding acquisition, Conceptualization. **Sanghan Lee:** Writing – review & editing, Supervision, Project administration, Funding acquisition, Conceptualization.

Declaration of competing interest

The authors declare that they have no known competing financial interests or personal relationships that could have appeared to influence the work reported in this paper.

Acknowledgments

S. Lee and H. W. Jeong contributed equally to this work. This work was supported by the Gwangju Institute of Science and Technology (GIST) research fund (Future-leading Specialized Research Project, 2025), the National Research Foundation of Korea, funded by the Ministry of Science and ICT (Grant Nos. 2020R1C1C100819315), and the GIST Advanced Institute of Instrumental Analysis (GAIA).

Appendix A. Supplementary data

Supplementary data to this article can be found online at https://doi.org/10.1016/j.matdes.2025.114130.

Data availability

Data will be made available on request.

References

[1] T.S. Böscke, S.t. Teichert, D. Bräuhaus, J. Müller, U. Schröder, U. Böttger, T. Mikolajick, Phase transitions in ferroelectric silicon doped hafnium oxide, Appl. Phys. Lett. 99 (2011) 112904, https://doi.org/10.1063/1.3636434.

[2] Q. Luo, Y. Cheng, J. Yang, R. Cao, H. Ma, Y. Yang, R. Huang, W. Wei, Y. Zheng, T. Gong, J. Yu, X. Xu, P. Yuan, X. Li, L. Tai, H. Yu, D. Shang, Q. Liu, B. Yu, Q. Ren, H. Lv, M. Liu, A highly CMOS compatible hafnia-based ferroelectric diode, Nat. Commun. 11 (2020) 1391, https://doi.org/10.1038/s41467-020-15159-2.

[3] M.H. Park, Y.H. Lee, H.J. Kim, Y.J. Kim, T. Moon, K.D. Kim, J. Müller, A. Kersch, U. Schroeder, T. Mikolajick, C.S. Hwang, Ferroelectricity and antiferroelectricity of doped thin HfO_2-based films, Adv. Mater. 27 (2015) 1811–1831, https://doi.org/10.1002/adma.201404531.

[4] H.A. Hsain, Y. Lee, G. Parsons, J.L. Jones, Compositional dependence of crystallization temperatures and phase evolution in hafnia-zirconia (HfxZr1−x)O2 thin films, Appl. Phys. Lett. 116 (2020) 192901, https://doi.org/10.1063/5.0002835.

[5] U. Schroeder, M.H. Park, T. Mikolajick, C.S. Hwang, The fundamentals and applications of ferroelectric HfO2, Nat. Rev. Mater. 7 (2022) 653–669, https://doi.org/10.1038/s41578-022-00431-2.

[6] J. Müller, T.S. Böscke, U. Schröder, S. Mueller, D. Bräuhaus, U. Böttger, L. Frey, T. Mikolajick, Ferroelectricity in simple binary ZrO_2 and HfO_2, Nano Lett. 12 (2012) 4318–4323, https://doi.org/10.1021/nl302049k.

[7] B.-T. Lin, Y.-W. Lu, J. Shieh, M.-J. Chen, Induction of ferroelectricity in nanoscale ZrO2 thin films on Pt electrode without post-annealing, J. Eur. Ceram. Soc. 37 (2017) 1135–1139, https://doi.org/10.1016/j.jeurceramsoc.2016.10.028.

[8] E.A. Scott, S.W. Smith, M.D. Henry, C.M. Rost, A. Giri, J.T. Gaskins, S.S. Fields, S. T. Jaszewski, J.F. Ihlefeld, P.E. Hopkins, Thermal resistance and heat capacity in hafnium zirconium oxide (Hf1–xZrxO2) dielectrics and ferroelectric thin films, Appl. Phys. Lett. 113 (2018) 192901, https://doi.org/10.1063/1.5052244.

[9] C.S. Hwang, Prospective of semiconductor memory devices: from memory system to materials, Adv. Electr. Mater. 1 (2015) 1400056, https://doi.org/10.1002/aelm.201400056.

[10] J. Muller, E. Yurchuk, T. Schlosser, J. Paul, R. Hoffmann, S. Muller, D. Martin, S. Slesazeck, P. Polakowski, J. Sundqvist, M. Czernohorsky, K. Seidel, P. Kucher, R. Boschke, M. Trentzsch, K. Gebauer, U. Schroder, T. Mikolajick, Ferroelectricity in HfO_2 enables nonvolatile data storage in 28 nm HKMG, in: 2012 Symposium on VLSI Technology (VLSIT), IEEE, Honolulu, HI, USA, 2012, pp. 25–26. doi: 10.1109/VLSIT.2012.6242443.

[11] M. Pesic, S. Knebel, M. Hoffmann, C. Richter, T. Mikolajick, U. Schroeder, How to make DRAM non-volatile? Anti-ferroelectrics: a new paradigm for universal

memories, in: 2016 IEEE International Electron Devices Meeting (IEDM), IEEE, San Francisco, CA, USA, 2016, pp. 11.6.1–11.6.4, https://doi.org/10.1109/IEDM.2016.7838398.
[12] H. Kim, K.S. Dae, Y. Oh, S. Lee, Y. Lee, S. Ahn, J.H. Jang, J. Ahn, A Simple strategy to realize super stable ferroelectric capacitor via interface engineering, Adv. Mater. Inter. 9 (2022) 2102528, https://doi.org/10.1002/admi.202102528.
[13] B.Y. Kim, I.S. Lee, H.W. Park, Y.B. Lee, S.H. Lee, M. Oh, S.K. Ryoo, S.R. Byun, K. D. Kim, J.H. Lee, D. Cho, M.H. Park, C.S. Hwang, Top electrode engineering for high-performance ferroelectric $Hf_{0.5}Zr_{0.5}O_2$ capacitors, Adv. Mater. Technol. 8 (2023) 2300146, https://doi.org/10.1002/admt.202300146.
[14] T. Francois, C. Pellissier, S. Slesazeck, V. Havel, C. Richter, A. Makosiej, B. Giraud, E.T. Breyer, M. Materano, P. Chiquet, M. Bocquet, L. Grenouillet, E. Nowak, U. Schroeder, F. Gaillard, J. Coignus, P. Blaise, C. Carabasse, N. Vaxelaire, T. Magis, F. Aussenac, V. Loup, Demonstration of BEOL-compatible ferroelectric Hf0.5 Zr0.5 O2 scaled FeRAM co-integrated with 130nm CMOS for embedded NVM applications, in: 2019 IEEE International Electron Devices Meeting (IEDM), IEEE, San Francisco, CA, USA, 2019, pp. 15.7.1–15.7.4, https://doi.org/10.1109/IEDM19573.2019.8993485.
[15] J. Okuno, T. Kunihiro, K. Konishi, M. Materano, T. Ali, K. Kuehnel, K. Seidel, T. Mikolajick, U. Schroeder, M. Tsukamoto, T. Umebayashi, 1T1C FeRAM memory array based on ferroelectric HZO with capacitor under bitline, IEEE J. Electron. Devices Soc. 10 (2022) 29–34, https://doi.org/10.1109/JEDS.2021.3129279.
[16] M.H. Park, Y.H. Lee, H.J. Kim, T. Schenk, W. Lee, K.D. Kim, F.P.G. Fengler, T. Mikolajick, U. Schroeder, C.S. Hwang, Surface and grain boundary energy as the key enabler of ferroelectricity in nanoscale hafnia-zirconia: a comparison of model and experiment, Nanoscale 9 (2017) 9973–9986, https://doi.org/10.1039/C7NR02121F.
[17] R. Materlik, C. Künneth, A. Kersch, The origin of ferroelectricity in Hf1−xZrxO2: a computational investigation and a surface energy model, J. Appl. Phys. 117 (2015) 134109, https://doi.org/10.1063/1.4916707.
[18] S. Mueller, J. Mueller, A. Singh, S. Riedel, J. Sundqvist, U. Schroeder, T. Mikolajick, Incipient ferroelectricity in Al-doped HfO_2 thin films, Adv. Funct. Mater. 22 (2012) 2412–2417, https://doi.org/10.1002/adfm.201103119.
[19] A. Chernikova, M. Kozodaev, A. Markeev, Yu. Matveev, D. Negrov, O. Orlov, Confinement-free annealing induced ferroelectricity in Hf0.5Zr0.5O2 thin films, Microelectron. Eng. 147 (2015) 15–18, https://doi.org/10.1016/j.mee.2015.04.024.
[20] S.J. Kim, D. Narayan, J.-G. Lee, J. Mohan, J.S. Lee, J. Lee, H.S. Kim, Y.-C. Byun, A. T. Lucero, C.D. Young, S.R. Summerfelt, T. San, L. Colombo, J. Kim, Large ferroelectric polarization of TiN/Hf0.5Zr0.5O2/TiN capacitors due to stress-induced crystallization at low thermal budget, Appl. Phys. Lett. 111 (2017) 242901, https://doi.org/10.1063/1.4995619.
[21] S.S. Fields, T. Cai, S.T. Jaszewski, A. Salanova, T. Mimura, H.H. Heinrich, M. D. Henry, K.P. Kelley, B.W. Sheldon, J.F. Ihlefeld, Origin of ferroelectric phase stabilization via the clamping effect in ferroelectric hafnium zirconium oxide thin films, Adv. Electr. Mater. 8 (2022) 2200601, https://doi.org/10.1002/aelm.202200601.
[22] R. Han, P. Hong, S. Ning, Q. Xu, M. Bai, J. Zhou, K. Li, F. Liu, F. Shi, F. Luo, Z. Huo, The effect of stress on HfO2-based ferroelectric thin films: a review of recent advances, J. Appl. Phys. 133 (2023) 240702, https://doi.org/10.1063/5.0146998.
[23] R. Cao, Y. Wang, S. Zhao, Y. Yang, X. Zhao, W. Wang, X. Zhang, H. Lv, Q. Liu, M. Liu, Effects of capping electrode on ferroelectric properties of $Hf_{0.5}Zr_{0.5}O_2$ thin films, IEEE Electron. Device Lett. 39 (2018) 1207–1210, https://doi.org/10.1109/LED.2018.2846570.
[24] H. Kim, A. Kashir, S. Oh, H. Hwang, A new approach to achieving strong ferroelectric properties in TiN/$Hf_{0.5}Zr_{0.5}O_2$/TiN devices, Nanotechnology 32 (2021) 055703, https://doi.org/10.1088/1361-6528/abc115.
[25] T.S. Böscke, J. Müller, D. Bräuhaus, U. Schröder, U. Böttger, Ferroelectricity in hafnium oxide thin films, Appl. Phys. Lett. 99 (2011) 102903, https://doi.org/10.1063/1.3634052.
[26] P. Jiang, Q. Luo, X. Xu, T. Gong, P. Yuan, Y. Wang, Z. Gao, W. Wei, L. Tai, H. Lv, Wake-up effect in HfO_2-based ferroelectric films, Adv. Electr. Mater. 7 (2021) 2000728, https://doi.org/10.1002/aelm.202000728.
[27] M.H. Park, Y.H. Lee, T. Mikolajick, U. Schroeder, C.S. Hwang, Review and perspective on ferroelectric HfO2-based thin films for memory applications, MRS Commun. 8 (2018) 795–808, https://doi.org/10.1557/mrc.2018.175.
[28] R. Alcala, M. Materano, P.D. Lomenzo, P. Vishnumurthy, W. Hamouda, C. Dubourdieu, A. Kersch, N. Barrett, T. Mikolajick, U. Schroeder, The electrode-ferroelectric interface as the primary constraint on endurance and retention in HZO-based ferroelectric capacitors, Adv. Funct. Mater. 33 (2023) 2303261, https://doi.org/10.1002/adfm.202303261.
[29] S.T. Jaszewski, S.S. Fields, S. Calderon, B.L. Aronson, T.E. Beechem, K.P. Kelley, C. Zhang, M.K. Lenox, I.A. Brummel, E.C. Dickey, J.F. Ihlefeld, Phase transformations driving biaxial stress reduction during wake-up of ferroelectric hafnium zirconium oxide thin films, Adv. Electr. Mater. 10 (2024) 2400151, https://doi.org/10.1002/aelm.202400151.
[30] Y. Cheng, Z. Gao, K.H. Ye, H.W. Park, Y. Zheng, Y. Zheng, J. Gao, M.H. Park, J.-H. Choi, K.-H. Xue, C.S. Hwang, H. Lyu, Reversible transition between the polar and antipolar phases and its implications for wake-up and fatigue in HfO2-based ferroelectric thin film, Nat. Commun. 13 (2022) 645, https://doi.org/10.1038/s41467-022-28236-5.
[31] P.D. Lomenzo, S. Slesazeck, M. Hoffmann, T. Mikolajick, U. Schroeder, B. Max, T. Mikolajick, Ferroelectric $Hf_{1-x}Zr_xO_2$ memories: device reliability and depolarization fields, in: 2019 19th Non-Volatile Memory Technology Symposium (NVMTS), IEEE, Durham, NC, USA, 2019, pp. 1–8, https://doi.org/10.1109/NVMTS47818.2019.9043368.
[32] D.-P. Xu, L.-J. Yu, X.-D. Chen, L. Chen, Q.-Q. Sun, H. Zhu, H.-L. Lu, P. Zhou, S.-J. Ding, D.W. Zhang, In situ analysis of oxygen vacancies and band alignment in HfO2/TiN structure for CMOS applications, Nanoscale Res. Lett. 12 (2017) 311, https://doi.org/10.1186/s11671-017-2068-y.
[33] Y. Zhang, Z. Fan, D. Wang, J. Wang, Z. Zou, Y. Li, Q. Li, R. Tao, D. Chen, M. Zeng, X. Gao, J. Dai, G. Zhou, X. Lu, J.-M. Liu, Enhanced ferroelectric properties and insulator–metal transition-induced shift of polarization-voltage hysteresis loop in VO_x-capped $Hf_{0.5}Zr_{0.5}O_2$ thin films, ACS Appl. Mater. Interfaces 12 (2020) 40510–40517, https://doi.org/10.1021/acsami.0c10964.
[34] T. Onaya, T. Nabatame, M. Inoue, T. Sawada, H. Ota, Y. Morita, Wake-up-free properties and high fatigue resistance of Hf x Zr1− x O2-based metal–ferroelectric–semiconductor using top ZrO2 nucleation layer at low thermal budget (300 °C), APL Mater. 10 (2022) 051110, https://doi.org/10.1063/5.0091661.
[35] Y. Goh, S.H. Cho, S.-H.-K. Park, S. Jeon, Oxygen vacancy control as a strategy to achieve highly reliable hafnia ferroelectrics using oxide electrode, Nanoscale 12 (2020) 9024–9031, https://doi.org/10.1039/D0NR00933D.
[36] J. Wang, M. Qin, M. Zeng, X. Gao, G. Zhou, X. Lu, J.-M. Liu, D. Wang, Q. Li, A. Zhang, D. Gao, M. Guo, J. Feng, Z. Fan, D. Chen, Excellent ferroelectric properties of Hf $_{0.5}$ Zr $_{0.5}$ O $_2$ thin films induced by Al $_2$ O $_3$ dielectric layer, IEEE Electron Device Lett. 40 (2019) 1937–1940, https://doi.org/10.1109/LED.2019.2950916.
[37] F. Mehmood, R. Alcala, P. Vishnumurthy, B. Xu, R. Sachdeva, T. Mikolajick, U. Schroeder, Reliability improvement from La_2O_3 interfaces in $Hf_{0.5}Zr_{0.5}O_2$-based ferroelectric capacitors, Adv. Mater. Inter. 10 (2023) 2202151, https://doi.org/10.1002/admi.202202151.
[38] A.K. Geim, I.V. Grigorieva, Van der Waals heterostructures, Nature 499 (2013) 419–425, https://doi.org/10.1038/nature12385.
[39] Y. Liu, X. Duan, Y. Huang, X. Duan, Two-dimensional transistors beyond graphene and TMDCs, Chem. Soc. Rev. 47 (2018) 6388–6409, https://doi.org/10.1039/C8CS00318A.
[40] S. Wang, X. Cui, C. Jian, H. Cheng, M. Niu, J. Yu, J. Yan, W. Huang, Stacking-engineered heterostructures in transition metal dichalcogenides, Adv. Mater. 33 (2021) 2005735, https://doi.org/10.1002/adma.202005735.
[41] G.H. Ahn, M. Amani, H. Rasool, D.-H. Lien, J.P. Mastandrea, J.W. Ager Iii, M. Dubey, D.C. Chrzan, A.M. Minor, A. Javey, Strain-engineered growth of two-dimensional materials, Nat. Commun. 8 (2017) 608, https://doi.org/10.1038/s41467-017-00516-5.
[42] S. Mueller, S. Slesazeck, T. Mikolajick, J. Muller, P. Polakowski, S. Flachowsky, Next-generation ferroelectric memories based on FE-HfO_2, in: 2015 Joint IEEE International Symposium on the Applications of Ferroelectric (ISAF), International Symposium on Integrated Functionalities (ISIF), and Piezoelectric Force Microscopy Workshop (PFM), IEEE, Singapore, 2015, pp. 233–236, https://doi.org/10.1109/ISAF.2015.7172714.
[43] M. Hyuk Park, H. Joon Kim, Y. Jin Kim, T. Moon, C. Seong Hwang, The effects of crystallographic orientation and strain of thin Hf0.5Zr0.5O2 film on its ferroelectricity, Appl. Phys. Lett. 104 (2014) 072901, https://doi.org/10.1063/1.4866008.
[44] R.R. Khakimov, A.G. Chernikova, A.A. Koroleva, A.M. Markeev, On the reliability of HZO-based ferroelectric capacitors: the cases of Ru and TiN electrodes, Nanomaterials 12 (2022) 3059, https://doi.org/10.3390/nano12173059.
[45] T.K. Paul, A.K. Saha, S.K. Gupta, Oxygen vacancy-induced monoclinic dead layers in ferroelectric HfO2 with metal electrodes, J. Appl. Phys. 137 (2025) 144102, https://doi.org/10.1063/5.0252663.
[46] P. Chaudhary, P. Buragohain, M. Kozodaev, S. Zarubin, V. Mikheev, A. Chouprik, A. Lipatov, A. Sinitskii, A. Zenkevich, A. Gruverman, Electroresistance effect in MoS2-Hf0.5Zr0.5O2 heterojunctions, Appl. Phys. Lett. 118 (2021) 083106, https://doi.org/10.1063/5.0035306.
[47] S.H. Kim, G.T. Yu, G.H. Park, D.H. Lee, J.Y. Park, K. Yang, E.B. Lee, J.I. Lee, M. H. Park, Interfacial engineering of a Mo/$Hf_{0.3}$ $Zr_{0.7}$ O_2 /Si capacitor using the direct scavenging effect of a thin Ti layer, Chem. Commun. 57 (2021) 12452–12455, https://doi.org/10.1039/D1CC04966F.
[48] K. Toprasertpong, K. Tahara, Y. Hikosaka, K. Nakamura, H. Saito, M. Takenaka, S. Takagi, Low operating voltage, improved breakdown tolerance, and high endurance in $Hf_{0.5}Zr_{0.5}O_2$ ferroelectric capacitors achieved by thickness scaling down to 4 nm for embedded ferroelectric memory, ACS Appl. Mater. Interfaces 14 (2022) 51137–51148, https://doi.org/10.1021/acsami.2c15369.
[49] F. Mehmood, M. Hoffmann, P.D. Lomenzo, C. Richter, M. Materano, T. Mikolajick, U. Schroeder, Bulk depolarization fields as a major contributor to the ferroelectric reliability performance in lanthanum doped $Hf_{0.5}Zr_{0.5}O_2$ capacitors, Adv. Mater. Inter. 6 (2019) 1901180. doi: 10.1002/admi.201901180.
[50] Y. Goh, S.H. Cho, S.-H.-K. Park, S. Jeon, Crystalline phase-controlled high-quality hafnia ferroelectric With RuO_2 electrode, IEEE Trans. Electron. Devices 67 (2020) 3431–3434, https://doi.org/10.1109/TED.2020.2998444.
[51] Y. Lee, Y. Goh, J. Hwang, D. Das, S. Jeon, The influence of top and bottom metal electrodes on ferroelectricity of hafnia, IEEE Trans. Electron Devices 68 (2021) 523–528, https://doi.org/10.1109/TED.2020.3046173.
[52] S. Lee, J.-G. Choi, S.H. Kim, W.-J. Lee, T. Kim, M.H. Park, M.-H. Yoon, Non-centrosymmetric crystallization in ferroelectric hafnium zirconium oxide via photon-assisted defect modulation, Mater. Sci. Eng. R. Rep. 159 (2024) 100800, https://doi.org/10.1016/j.mser.2024.100800.
[53] H. Lee, K.S. Chang, Y.J. Tak, T.S. Jung, J.W. Park, W.-G. Kim, J. Chung, C.B. Jeong, H.J. Kim, Electric field-aided selective activation for indium-gallium-zinc-oxide thin film transistors, Sci. Rep. 6 (2016) 35044, https://doi.org/10.1038/srep35044.

[54] S. Im, S.-Y. Kang, Y. Kim, J.H. Kim, J.-P. Im, S.-M. Yoon, S.E. Moon, J. Woo, Ferroelectric switching in trilayer Al2O3/HfZrOx/Al2O3 structure, Micromachines 11 (2020) 910, https://doi.org/10.3390/mi11100910.
[55] H.M.I. Jaim, S. Lee, X. Zhang, I. Takeuchi, Stability of the oxygen vacancy induced conductivity in BaSnO3 thin films on SrTiO3, Appl. Phys. Lett. 111 (2017) 172102, https://doi.org/10.1063/1.4996548.
[56] K.H. Ye, T. Jeong, S. Yoon, D. Kim, C.S. Hwang, J.-H. Choi, Theoretical understanding of the in-plane tensile strain effects on enhancing the ferroelectric performance of $Hf_{0.5}$ $Zr_{0.5}$ O_2 and ZrO_2 thin films, Nanoscale 17 (2025) 540–551, https://doi.org/10.1039/D4NR03333G.
[57] K. Chae, A. Kummel, K. Cho, DFT models of ferroelectric hafnium-zirconium oxide stacks with and without dielectric interlayers, in: 2021 International Symposium on VLSI Technology, Systems and Applications (VLSI-TSA), IEEE, Hsinchu, Taiwan, 2021, pp. 1–2, https://doi.org/10.1109/VLSI-TSA51926.2021.9440127.
[58] Y.-W. Chen, C.W. Liu, Boost of orthorhombic population with amorphous SiO_2 interfacial layer—a DFT study, Semicond. Sci. Technol. 37 (2022) 05LT01, https://doi.org/10.1088/1361-6641/ac5a5e.
[59] M.S. Ullah, A.H.B. Yousuf, A.D. Es-Sakhi, M.H. Chowdhury, Analysis of optical and electronic properties of MoS2 for optoelectronics and FET applications, in: Lakeland, FL, USA, 2018, p. 020001. doi: 10.1063/1.5034320.
[60] H. Lin, J. Ou, Z. Fan, X. Yan, W. Hu, B. Cui, J. Xu, W. Li, Z. Chen, B. Yang, K. Liu, L. Mo, M. Li, X. Lu, G. Zhou, X. Gao, J.-M. Liu, In situ training of an in-sensor artificial neural network based on ferroelectric photosensors, Nat. Commun. 16 (2025) 421, https://doi.org/10.1038/s41467-024-55508-z.